



# Residual stress effects during additive manufacturing of reinforced thin nickel–chromium plates

Eann A. Patterson<sup>1</sup> · John Lambros<sup>2</sup> · Rodrigo Magana-Carranza<sup>1</sup> · Christopher J. Sutcliffe<sup>3</sup>

Received: 25 May 2022 / Accepted: 5 October 2022 / Published online: 22 October 2022  
© The Author(s) 2022

## Abstract

Additive manufacturing (AM) is a powerful technique for producing metallic components with complex geometry relatively quickly, cheaply and directly from digital representations; however, residual stresses induced during manufacturing can result in distortions of components and reductions in mechanical performance, especially in parts that lack rotational symmetry and, or have cross sections with large aspect ratios. Geometrically reinforced thin plates have been built in nickel–chromium alloy using laser-powder bed fusion (L-PBF) and their shapes measured using stereoscopic digital image correlation before and after release from the base-plate of the AM machine. The results show that residual stresses cause potentially severe out-of-plane deformation that can be alleviated using either an enveloping support structure, which increased the build time substantially, was difficult to remove and wasted material, or using buttress supports to the reinforced edges of the thin plate. The buttresses were quick to build and remove, minimised waste but needed careful design. Plates built in a landscape orientation required out-of-plane buttresses while those built in a portrait orientation required both in-plane and out-of-plane buttresses. In both cases, out-of-plane deformation increased on release from the baseplate but this was mitigated by incremental release which resulted in out-of-plane deformations of less than 5% of the in-plane dimensions.

**Keywords** Additive manufacturing · Residual stresses · Thin plates · Out-of-plane deformation · Digital image correlation

## 1 Introduction

Additive manufacturing (AM) is a modern technique for producing engineering components in a variety of materials including metals, plastics and composites. Many types of additive manufacturing are available; however, their common feature is the creation of parts in a layer-by-layer, or slice-by-slice, process based on a digital representation of the engineering component or part. A key advantage of additive manufacturing is the capability to produce a part with a complex geometry without part-specific tooling, such as the moulds and dies needed in casting and forging, and without wasting large amounts of material as in machining or

subtractive manufacturing. However, stresses induced during additive manufacturing can result in distortion and ultimately reduce the mechanical performance of parts. These stresses, known as residual stresses, have been the subject of investigations since additive manufacturing was first introduced for manufacturing prototypes (for example, Curtis et al. [1]). For many parts with some level of rotational symmetry, the distribution of residual stresses will also possess a degree of symmetry that will prevent significant distortion of the part although may still influence mechanical properties such as strength and failure. Parts with substantial cross sections may also not exhibit significant shape distortion due to the stiffness of the part containing the residual stresses. However, parts that lack rotational symmetry and, or have cross-sections with large aspect ratios (i.e. in-plane to out-of-plane dimensions) are likely to be particularly susceptible to distortion caused by the residual stresses generated during additive manufacturing. One class of such parts has been investigated here, namely thin rectangular plates with geometrically reinforced edges made using a metallic alloy with a high resistance to temperature. This geometry is of interest because it is representative of panels used to contain plasma

✉ Eann A. Patterson  
eann.patterson@liverpool.ac.uk

<sup>1</sup> Department of Mechanical, Materials & Aerospace Engineering, University of Liverpool, Liverpool, UK

<sup>2</sup> Department of Aerospace Engineering, University of Illinois, Urbana-Champaign, USA

<sup>3</sup> Meta Consulting LDA, Lisbon, Portugal

in fusion reactors and of the skin of hypersonic flight vehicles [2–4]. The number of devices manufactured for both of these applications is likely to be small and hence additive manufacturing is a potentially attractive option for producing parts and provides the motivation for this study.

The influence of residual stresses may be thought of as occurring at three different length scales in metals [5]. At the macroscale, non-uniform plastic deformation sets up differential strains within a component that create macrostresses that act on the scale of the geometry of the component to cause global distortion. At the microscale, local microstructural effects and phase transformations generate micro-stresses which can influence the material properties of the component. And at the atomic scale, residual stresses can be induced by heterogeneous behaviour [6, 7]. Macroscale residual stresses have been the primary focus of attention in additive manufacturing due to their tendency to cause part distortions and the possibility of alleviating their effects through changes in the process parameters. It is difficult to measure residual stresses in metals directly; however, X-ray diffraction [8, 9] and neutron diffraction [10] have been used to evaluate residual strains in additively manufactured parts following completion of the build. Magana-Carranza et al. [11, 12], who also reviewed residual stresses induced by additive manufacturing, have used a force transducer device incorporated into an AM machine to measure forces induced during the build process in order to enhance understanding of the development of macroscale residual stresses. They studied the laser-powder bed fusion (L-PBF) process [13, 14] and concluded that laser scanning strategies with shorter vectors tended to induce higher levels of force which were sensitive to the laser power and point distance when the energy density delivered to the part was below a critical value. These findings resolved some apparently

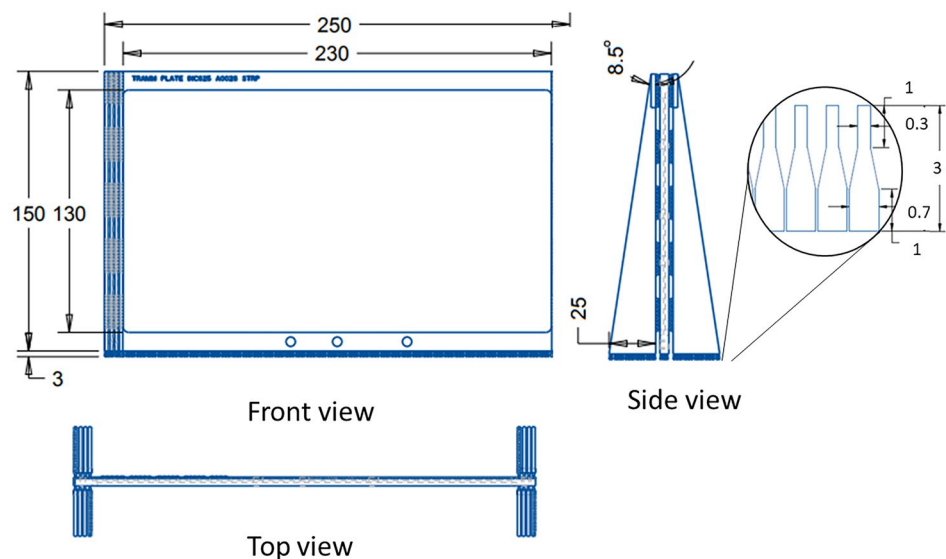
contradictory evidence from simulations and post-build measurements thus providing some confidence to attempt to build thin plates which are susceptible to deformation due to residual stress even when built using subtractive manufacturing [8]. This confidence was perhaps misplaced since many attempts were required before an acceptable part was built, as outlined below. Nevertheless, the study has resulted in a series of conclusions that should be relevant when building this type of part using additive manufacturing and laser-powder bed fusion in particular.

## 2 Methods

### 2.1 Geometrically reinforced plate

The specific motivation of the study was to build, using additive manufacturing, thin rectangular plates with reinforced edges that could be used in a study of their response to thermo-acoustic excitation and compare the results to plates of identical geometry subtractively machined from a thick plate stock [4]. As mentioned above, the choice of a reinforced thin-plate geometry was motivated by applications in fusion powerplants and hypersonic flight vehicles. The details of the geometry of the reinforced plate are shown in Fig. 1 and consist of a 1-mm-thick flat plate with in-plane dimensions of 130 mm and 230 mm surrounded by a reinforcing edge, or frame, of 10 mm  $\times$  5 mm rectangular cross section. The frame contained a number of holes that were designed for use in the thermo-acoustic excitation experiments and also had the specification of the plate embossed on the top left corner as shown in Fig. 1. Note the presence of supporting structures around the reinforced plate in Fig. 1. Details of these supports will be provided in

**Fig. 1** Geometry of edge-reinforced thin plates showing the design of the out-of-plane buttresses that were attached in latter builds to the edges of geometric reinforcement or frame. All dimensions in mm



subsequent sections. All of the reinforced plates were built using a nickel–chromium alloy (Inconel 625) in the form of gas-atomised powder (Carpenter Additive, UK) which is widely used for additive manufacturing employing L-PBF. A material datasheet for this powder is available from the supplier [15].

## 2.2 L-PBF

L-PBF uses a laser beam to selectively melt sections of a thin layer of metal powder on a flatbed in an inert atmosphere [9]. A three-dimensional part is built layer-by-layer with a thin layer of powder spread over the previous layer at each stage. The initial layer is built on the baseplate of the machine which is typically pre-heated to reduce residual stresses generated by differential strains in the baseplate and lower layers of the part. Residual stresses are generated during the L-PBF process as a result of the thermal gradient mechanism that occurs around the spot where the laser beam is incident on the part and causes local heating or melting of the upper layer(s) of the part followed by rapid cooling with a steep temperature gradient when the laser beam moves away [10].

Manufacturing of the geometrically reinforced plates was performed using a L-PBF machine (Renishaw AM250, UK) with a maximum laser power of 1 kW. In all builds the laser power was 400 W, the exposure time 40  $\mu$ s, the point distance 70  $\mu$ m, and the layer thickness 60  $\mu$ m. These values for the processing parameters were chosen based on prior

experience [7] and to achieve a density in the parts greater than 99% of the cast material. The density was measured in ten cubes with side length of 10 mm using Archimedes' principle and was found to have a mean of 99.64% with a standard deviation of 0.42% relative density.

Initially two half-size (65 mm  $\times$  115 mm) test plates, with the same thicknesses as shown in Fig. 1, were built to establish whether to use the Meander or Stripes scan strategy (shown in Fig. 2) for these thin section parts. The build times for these plates were 5 h 8 min and 4 h 32 min, respectively, using the Meander and Stripes scan strategies. The resultant out-of-plane measurements across a diagonal for each of the two test plates after release from the baseplate are shown in Fig. 3, with details of how the measurements were made presented in the next section. It can be seen in Fig. 3 that the Stripes scan strategy produced less curvature by a factor of 2, and hence, it was used in all subsequent builds in this study. This result is consistent with the results from our earlier study from which we concluded that scan strategies with shorter scan vectors generate lower residual stresses [7].

The reinforced plates were built on the standard baseplate for the machine. Previous studies suggest that a pre-heated substrate, to 160  $^{\circ}$ C [16] or to 180  $^{\circ}$ C [17], reduced the temperature gradients within the parts and decreased residual stresses; therefore, the base plate was heated to 170  $^{\circ}$ C, which was the maximum temperature permitted by the machine's control system. The dimensions of the baseplate and the reinforced plates required the latter to be orientated across the diagonal of the former when built in landscape

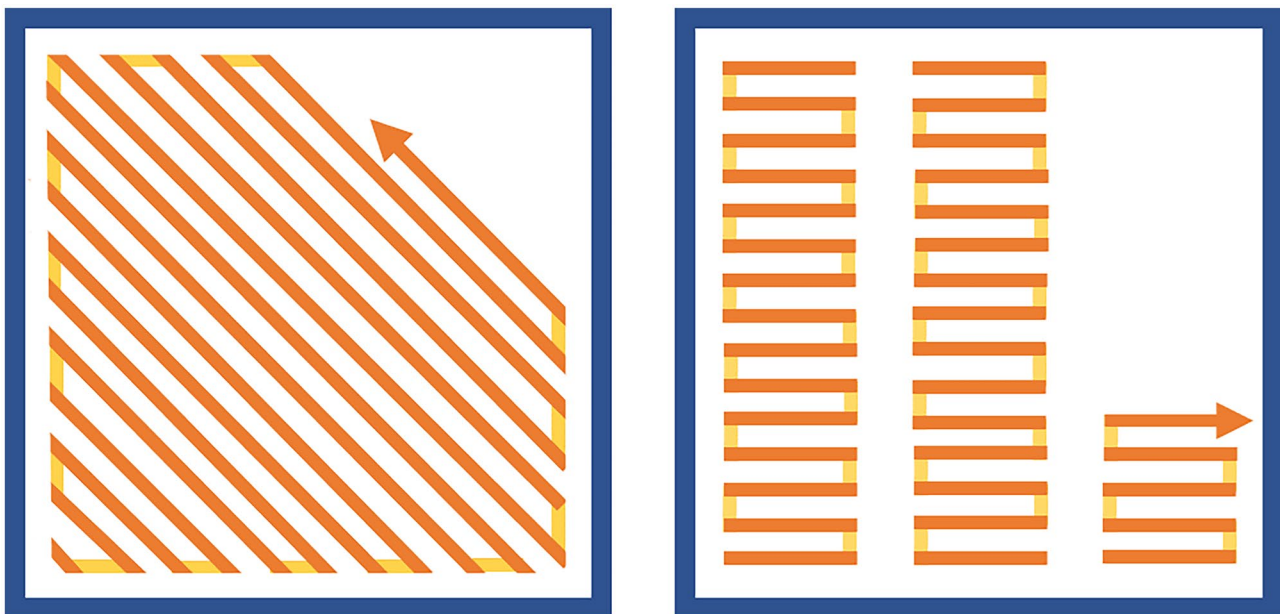


**Fig. 2** Schematic layout of Meander (left) and Stripes (right) scan strategy; the orange colors show the scan path and the deeper color indicates where the laser is switched on

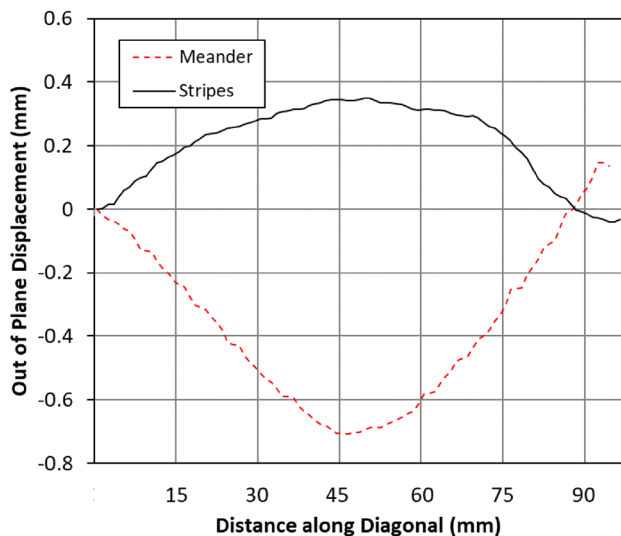


**Fig. 3** Z-measurements acquired using digital image correlation (DIC) along a diagonal of two test plates ( $115 \times 65 \times 1$  mm) with edge-reinforcements showing that the Stripes scan strategy produces a shape that deviates less from a plane

orientation, i.e. with the long side horizontal, and the same arrangement across the diagonal was maintained when the parts were built in portrait orientation, i.e. with the short side horizontal. A 3-mm high support structure consisting of a series of tapered rods as shown in Fig. 1 was built to separate the part from the baseplate and allow it to be detached after the build process. On completion of a build cycle, the baseplate was removed from the machine and the shape of the reinforced plate measured using stereoscopic digital image correlation, as described below, before progressively removing the reinforced plate from the baseplate by cutting through the supporting rods. In some cases, this removal proceeded in incremental stages with measurements made of the change in shape for each stage using the digital image correlation system.

### 2.3 Stereoscopic digital image correlation

The shapes of the plates were measured using a stereoscopic digital image correlation (DIC) system (Q400, Dantec Dynamics GmbH, Ulm, Germany). This system is capable of providing data on the shape of the plate relative to a plane or the displacements of the surface of the plate relative to an initial state [18]. In this study, it was used in both modes with the former datasets referred to as shape or z-measurements while the latter as out-of-plane displacements. The system was set up, as shown in the plan view in Fig. 4, to achieve a spatial resolution of 20 pixels/mm using a pair of identical CCD cameras with  $1292 \times 964$  pixels and 50 mm lenses.

At the end of each build process, the thin plate was painted black and then sprayed with white paint to form a speckle pattern to support the image correlation process which was performed using the software provided with the system (Istra 4D, Dantec Dynamics GmbH). A typical speckle pattern is shown inset in Fig. 4. The image correlation was performed using square facets or sub-images with sides of length 29 pixels whose centres had a pitch of 15 pixels.

Before each set of measurements was acquired, the system was calibrated using a calibration target (AI-08-BMB-9 X 9) supplied by the instrument manufacturer. In addition, the measurement uncertainty was estimated by taking an initial image of the plate before removal from the baseplate and then replacing it at the same position with the aid of positioning guides, capturing another image and correlating the two images. A typical result for out-of-plane displacement resulting from the correlation of two such pairs of images is shown as an inset in Fig. 4. This process was repeated six times for each plate. The resultant correlation maps provide an estimate of the measurement uncertainty which typically had a mean of zero and standard deviation of 0.0014 mm, i.e. there was no bias and a very low value of random noise.

On completion of a build process and after spray-painting the reinforced plate, the baseplate from the AM machine with the reinforced plate attached was placed on an optical table for the DIC measurements. The accuracy with which the baseplate could be relocated was within the measurement uncertainty of the digital image correlation system, as explained above. Pairs of stereoscopic images were recorded for the reinforced plate attached to the baseplate and subsequently as the supports were released which allowed the initial and final shapes of the reinforced plate to be evaluated as well as the evolution of out-of-plane displacements as it was released.

## 3 Results

After the reduced-scale test plates had been used to confirm that the Stripes scan strategy produced lower levels of deformation, an attempt was made to build a full-scale plate as described by the CAD drawing in Fig. 1, i.e. in landscape orientation with the long sides horizontal. This was not successful because the plate developed an S-shape profile as shown in the photograph of the completed build in Fig. 5. The shape of this plate was measured using the DIC system following its complete removal from the baseplate and the results are shown in Fig. 6. The lower three-quarters of the plate developed an approximately elliptical dome; however, at a height of about 105 mm a sudden change in behaviour occurred with a two-dimensional out-of-plane curve appearing.

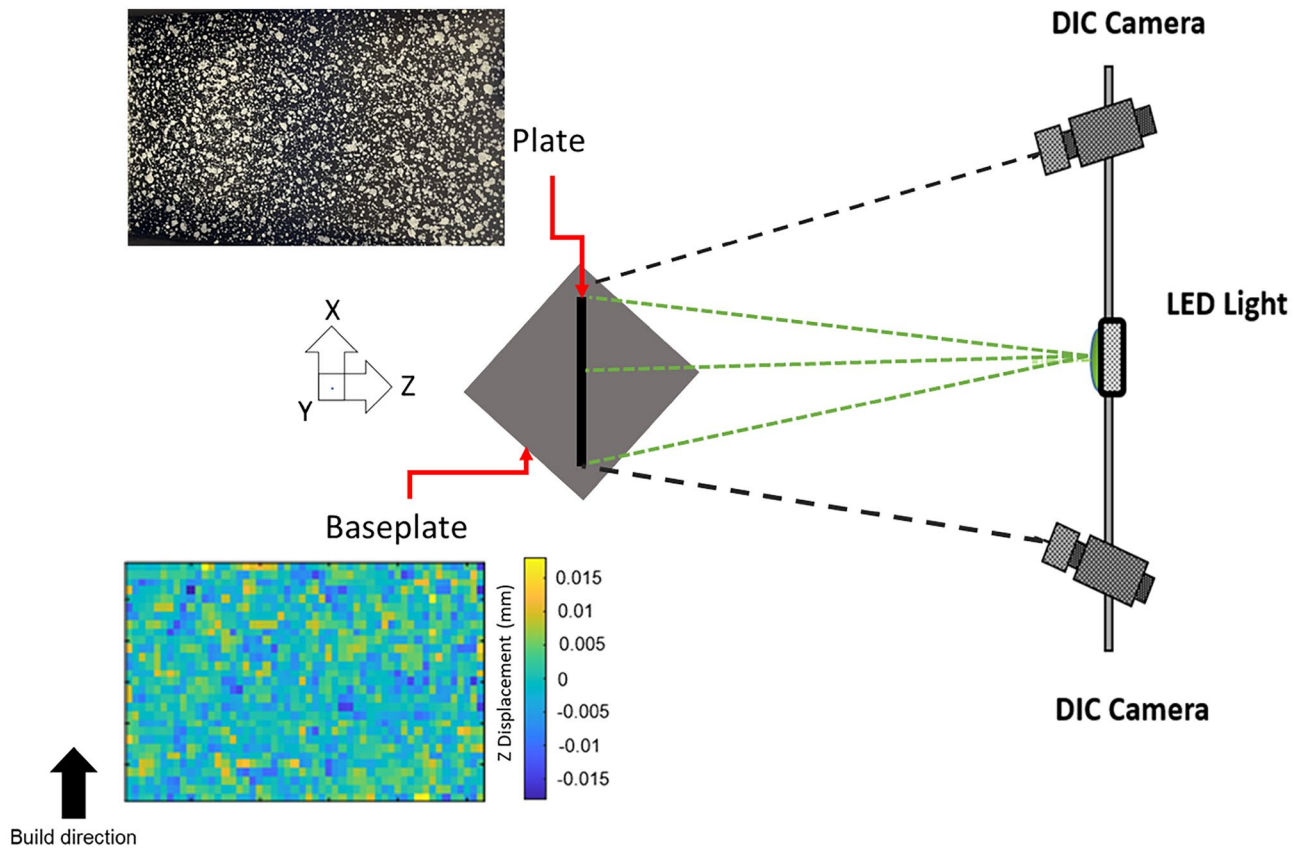


**Fig. 4** Schematic diagram of experimental set up for measuring out-of-plane displacements and shape of thin plates using digital image correlation together with insets showing a typical speckle pattern (top) and map of measurement uncertainty (bottom) for the 130×230 mm thin plate

A repeat of the process used to build the plate shown in Fig. 5 produced an identical plate. When two plates were built without the edge-reinforcement of the frame, a similar result was produced but with a delamination or split appearing horizontally between build layers at the height at which the out-of-plane curvature commenced, i.e. about 100 mm. Hence, it was decided to provide an additional support structure around the reinforced plate to stiffen and strengthen it during the AM build process. The design and completed build for the additional support structure are shown in Fig. 7. The completed build was removed from the baseplate and then the additional support structure was removed. The latter was a substantial task which was undertaken using an electric discharge machine; however, the resultant thin plate had a flatness of only 5.05 mm and its shape is shown in Fig. 6. Metrologically, flatness is defined as the minimum distance between two planes within which all the points on a surface lie [19].

The time required to remove the additional support structure shown in Fig. 7 and the material wasted probably negated the advantage gained from using additive manufacturing; hence, an alternative strategy was sought. The additional support structure was reduced to buttresses

supporting the vertical portion of the edge-reinforcements. These buttresses were triangular in their plane perpendicular to the plane of the reinforced-plate with their outside edge subtending an angle of  $8.5^\circ$  to the vertical and their inside edge attached to the edge reinforcement via small rods identical to those used to attach the structure to the baseplate, as shown in Fig. 1. Two plates were built separately with this geometry and the buttresses were removed, before each plate was removed from the base plate progressively by cutting the rod supports in increments alternating between the left and right side. For one plate the increments were 15 mm and for the other plate the increments were 5 mm. After each incremental cut, the baseplate was relocated on the optical table and a pair of stereoscopic images recorded which allowed the displacement of the thin plate to be monitored as it was released from the baseplate. The final shapes for these plates are shown in Fig. 8 which shows that the plate released in smaller increments had a slightly lower flatness of 5.5 mm; hence, the out-of-plane displacements during release of this plate are shown in Fig. 9.

The use of buttresses to provide support to the vertical portion of the edge-reinforcement or frame resulted in successful build processes but a flatness that was about 10%



**Fig. 5** Example of a build that failed for a thin plate without additional support shown in Fig. 1 and shape data in the top of Fig. 6

worse than using the additional support structure shown in Fig. 7. Therefore, it was decided to investigate building the plates in a portrait orientation, i.e. with their short side

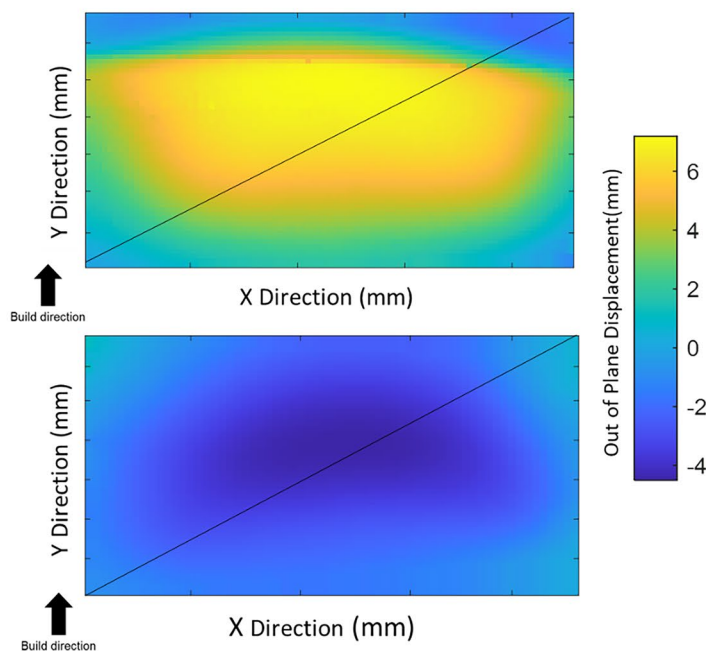
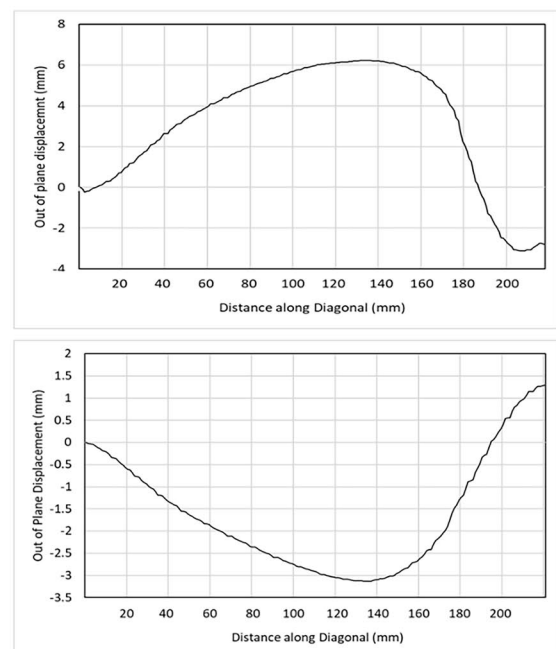


**Fig. 6** Shape of the front face of the edge-reinforced landscape plates built without any supporting structure (top) as shown in Fig. 5 and using an additional support system (bottom) as shown in Fig. 7 following removal from the baseplate. The maximum deviation from a

horizontal, and with buttresses of the same triangle ratio providing out-of-plane support during the build process. This strategy was unsuccessful and resulted in a delamination appearing between build layers at a height of about 230 mm or about 20 mm from the end of the build, as shown in Fig. 10 (left). However, the addition of in-plane buttresses solved this problem resulting in a successful build, also shown in Fig. 10 (centre and right). This successful build was released from the baseplate in alternate increments of 5 mm which resulted in a flatness of 4.6 mm as shown in Fig. 11. The out-of-plane displacements during the incremental release from the baseplate are shown in Fig. 12.

## 4 Discussion

The formation of residual stresses and the development of the shape of an edge-reinforced plate are history-dependent and time-varying processes in which the equilibrium of forces in the plate changes during the build process due to the addition of mass to the plate and due to energy transfers from the laser and to the surroundings. The equilibrium state also changes during the removal of the built part from the baseplate and when any additional supporting structure is removed. The sequence of out-of-plane displacement fields shown in Figs. 9 and 12 illustrate the changing state of the equilibrium of forces during release from the baseplate which results in changes to the shape of the part. However,



flat plane is 5.05 mm. For the plate built with an additional support system, the maximum deviation from a flat plane is 5.05 mm which does not occur along the diagonal plotted in the graphs on the right

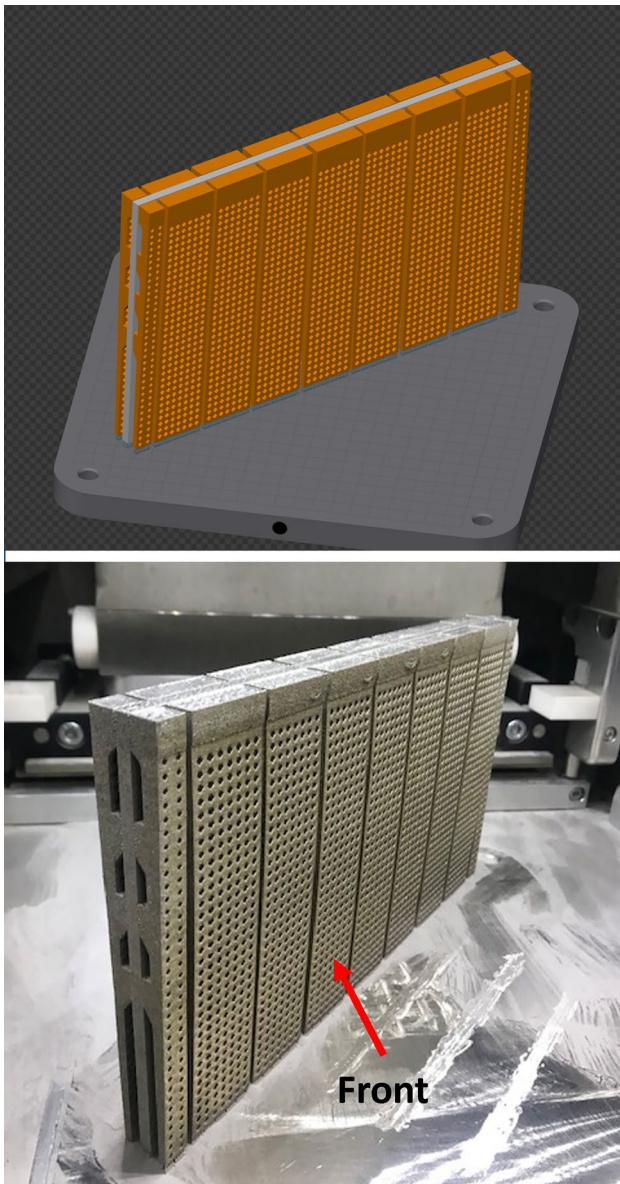


**Fig. 7** Three-dimensional rendering showing thin plate ( $230 \times 130 \times 1$  mm) in gray and total support structure in orange (top) and photograph of completed build attached to baseplate (bottom). See Fig. 6 for resultant geometry of edge-reinforced plate

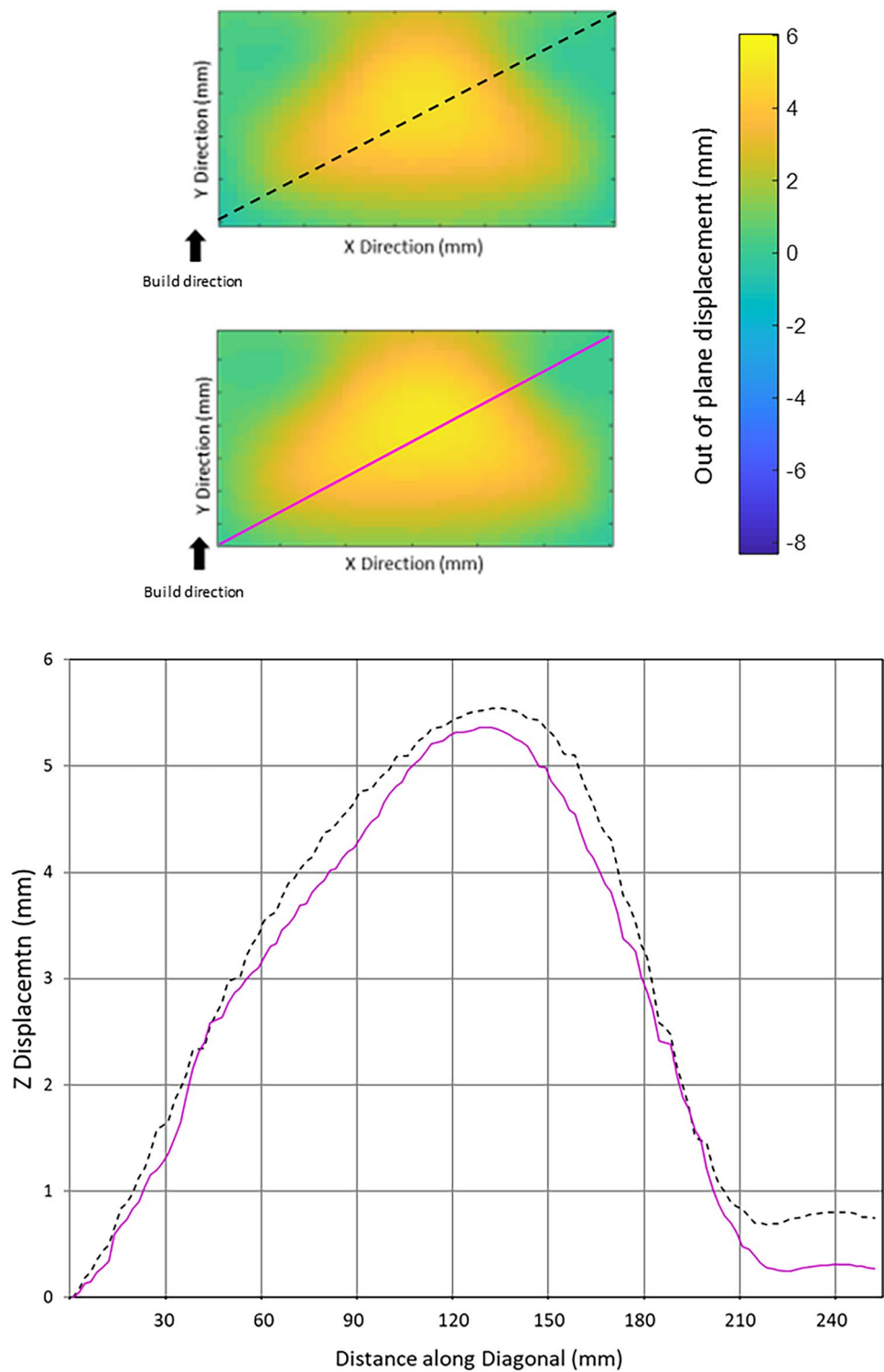
it is very difficult to monitor directly the changing balance of forces during the build in the chamber of the AM machine. In previous work, the authors have used a force transducer device fitted into the baseplate of an AM machine to monitor the time-varying response of the forces on the baseplate during the build process [6, 7]. It was found that the forces induced in the early stages of the build represented about 80% of the maximum force induced and relatively low levels of relaxation occurred during the scanning by the laser,

which implies that significant residual stress was locked into the part. In later stages of the build, the magnitude of forces induced and relaxed as each layer was added were approximately equal, which implies that the level of residual stress locked into the upper layers of the part was substantially less than for the lower layers adjacent to the baseplate. These observations were made on parts that were square in the horizontal plane scanned by the laser, i.e. had an aspect ratio of one compared to 50 for the reinforced edge of the thin plates, and had a height of the same order of magnitude as the reinforced edge of the plates in this study. Nevertheless, they help to explain both the substantial changes in shape that occurred in this research when the reinforced plates were released from the baseplate and the importance of the rate and pattern of release.

In the early stages of the build process, significant residual stresses are induced by the differential thermal expansion both within the part and between the part and the baseplate, during which the mechanical constraint from the baseplate is significant. Previous studies have found compressive residual forces in the centre of parts and tensile forces at the edges [4, 6], and this distribution of forces at the interface of the part with the baseplate is probably responsible for distribution of out-of-plane displacements along the bottom horizontal edge of the reinforced plates following release from the baseplate, as shown in Figs. 9 and 12.

It is important to consider that the shapes shown in Figs. 5 and 10 were developed layer-by-layer as the part was built. As the part height is built up, the influence of the baseplate constraint is likely to be diminished, while the reinforcement of the part by its frame may become more important. The influence of the reinforced edge was investigated by building two thin plates ( $230 \times 130$  mm) without the reinforced edge and with plate thicknesses of 1 mm and 1.2 mm. A delamination appeared in the thinner of the two plates at 93 mm above the baseplate and the thicker plate formed an out-of-plane S-shaped curve similar to the edge-reinforced plate in Fig. 5 but starting 108 mm above the baseplate compared to 100 mm when the edge-reinforcement was present. The development of a delamination between layers in the 1 mm thick plate when the edge reinforcement was absent suggests that the reinforcement was providing additional strength to the plate during the build process. Similar behaviour was observed in the plates built in portrait orientation without in-plane buttresses when delamination occurred, whereas for those plates with in-plane buttresses there was no delamination, as shown in Fig. 10. Previous work has concluded that residual stresses tends to be compressive in the centre of a layer and tensile at the edges [4, 6] which will cause bending of a layer into a catenary with the ends of the layer bending upwards, towards the laser. It is difficult to identify a trigger for the delaminations at a specific height in the build;

**Fig. 8** Shape measured using digital image correlation in edge-reinforced landscape plates built with additional buttresses (shown in Fig. 1) and removed from the baseplate in alternating 5 mm (top color map) and 15 mm (bottom color map) increments together with z-coordinate profiles (bottom) across diagonals (flatness was 5.5 and 5.69 mm, respectively)



however, it could be related to the rate of cooling, which will change as the mass of the part increases and alters both the heat capacity and conduction paths of the part. It might also be related to a misalignment of layers causing a new layer to be incompletely bonded to the previous one. It can be seen in Fig. 10 that there are small horizontal discontinuities

in the surface of the plate built without in-plane buttresses at heights of 113 and 225 mm above the baseplate. Data on the shape of the plate during the build process are not available; however, data at the completion of build and prior to removing the edge-reinforced plate from the baseplate are shown as the first step in Figs. 9 and 12 as part of the



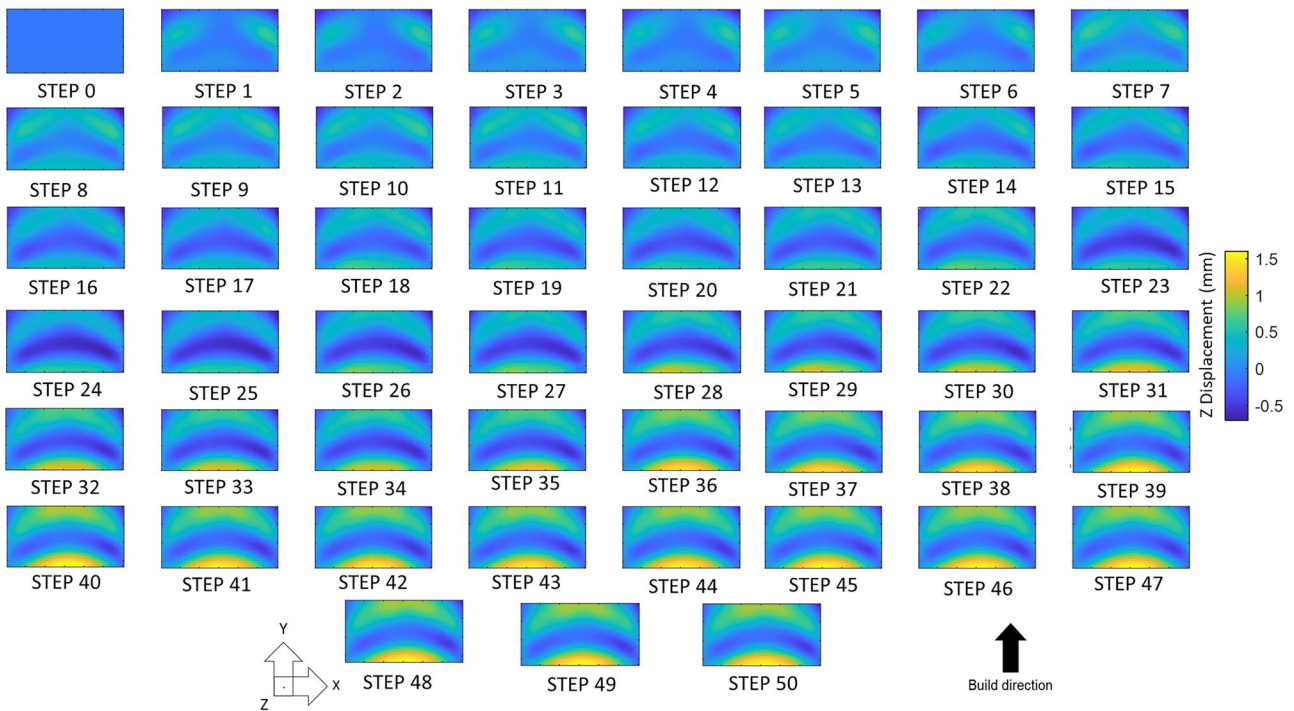


**Fig. 9** Out-of-plane displacements measured at each increment of 5 mm release from baseplate (odd numbers on right) for edge-reinforced landscape plate with additional buttresses (see geometry in Fig. 8). The dis-

placements are relative to initial shape of the plate on the baseplate at the end of the build cycle and measured on the front face (step 0)

sequence of changes on release from the baseplate and on a large scale in Fig. 11 for the plate built in portrait orientation. Hence, it can be postulated that these out-of-plane displacements move the top layer of the plate horizontally away from the path of the laser, which means the next layer is not built directly aligned with previous layers but effectively

over-hangs the previous layer resulting in an incomplete bonding of the layers that allows delamination to occur when cooling of the subsequent layers induces deformation into a catenary. In the absence of sufficient reinforcement, the stresses associated with the deformation into a catenary cause the plate to delaminate. For the plates built in the

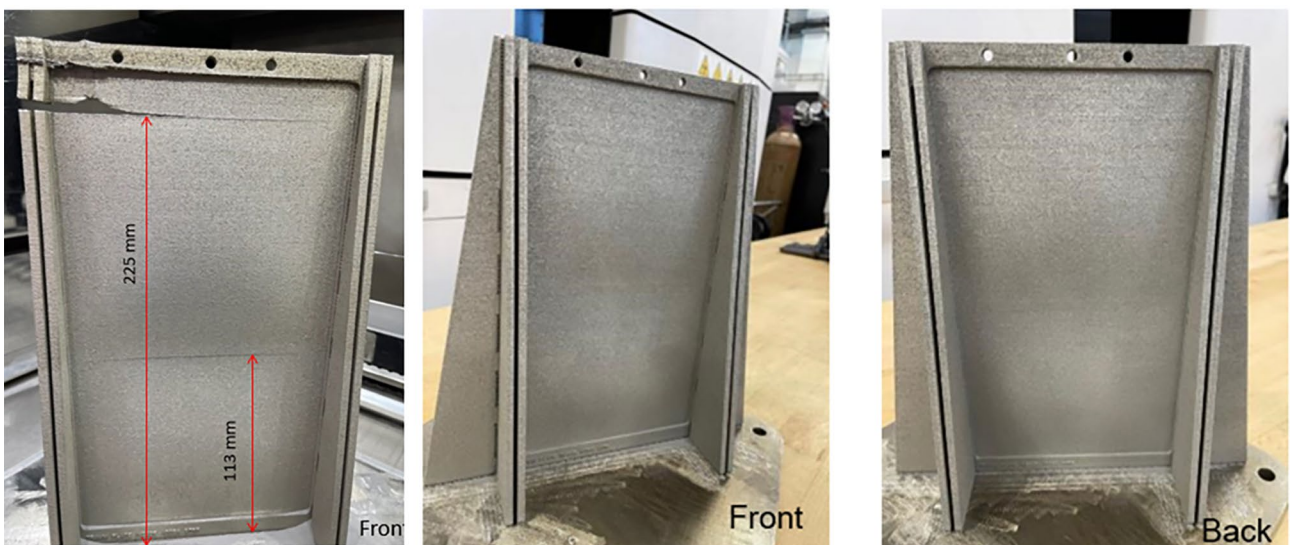


**Fig. 10** Completed builds of edge-reinforced plates built in portrait orientation without in-plane buttresses (left) leading to delamination and with in-plane buttresses (center and right) resulting in a successful build

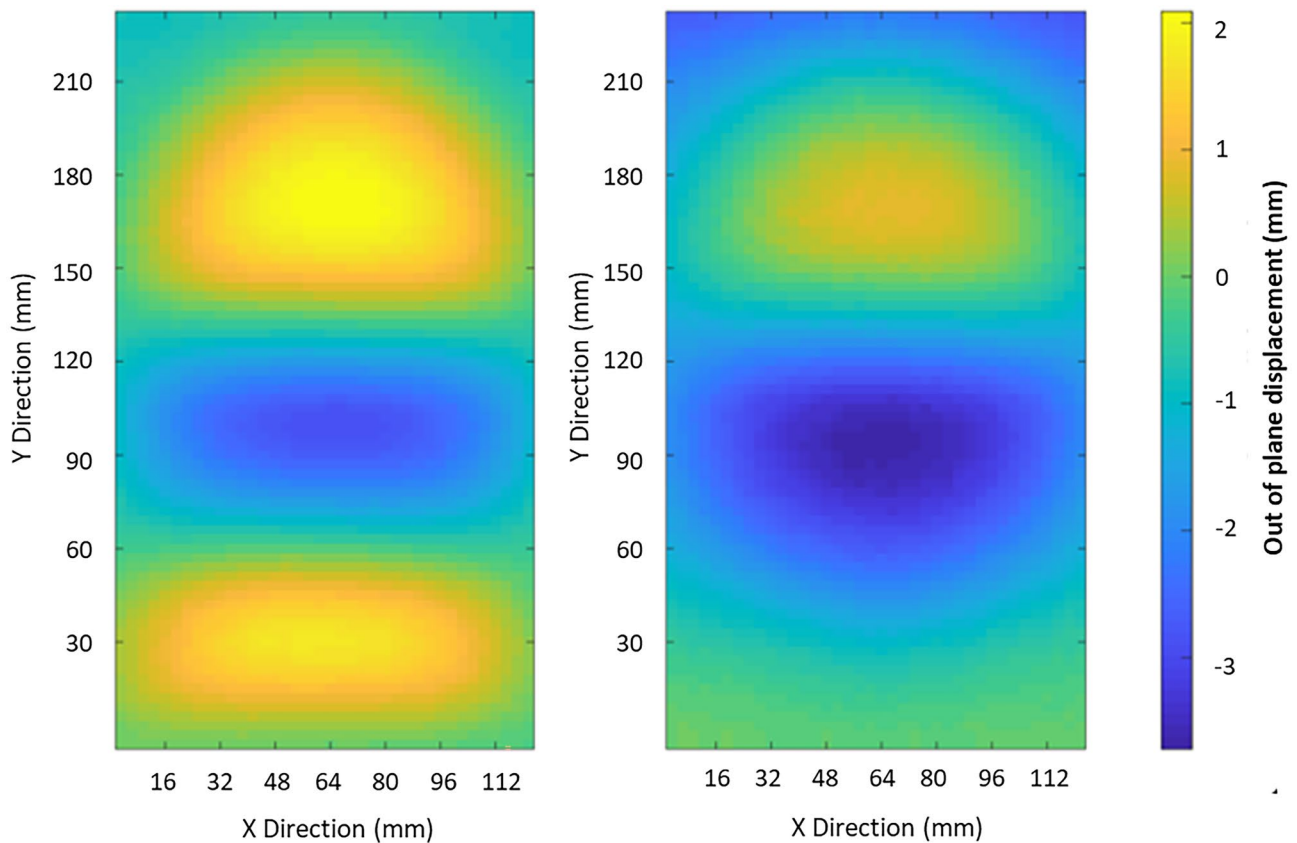


**Fig. 11** Shapes before (left) and after (right) release from baseplate for edge-reinforced plate ( $130 \times 230 \times 1$  mm) built in portrait orientation with in-plane and out-of-plane buttress (see Fig. 1) and with alternating incremental release from baseplate

landscape orientation, the reinforced edge is sufficient to resist delamination because only the plate without the edge reinforcement was seen to develop a delamination. However, for the plates built in the portrait orientation, both in-plane and out-of-plane buttresses were required to prevent delamination as shown in Fig. 10. The size of the AM machine's build platform prevented in-plane buttresses being used in the landscape orientation.

When a delamination does not initiate then it would seem that top edge of the partially built plate tends to translate out-of-plane due to the differential thermal strains in the plate. This might be a result of the additional constraint of the reinforcement inducing out-of-plane rather than in-plane deflection. The resultant misalignment of the top layer and next layer to be built results in a slight offset creating the beginning of the curved shape seen in Fig. 5. At a later stage in the build the reinforced plate starts to deflect in the opposite out-of-plane direction causing the just-built layer to realign under the path of the laser so that the s-shaped curve is formed. The reason for the realignment is difficult to surmise. These out-of-plane displacements during the build were prevented by including additional out-of-plane reinforcement, initially in the form of the total support structure

shown in Fig. 7, and then using the buttresses shown in Figs. 1 and 10.

The flatness of the edge-reinforced plates built in both landscape and portrait orientation with out-of-plane buttresses is about 2 mm when they are attached to the baseplate of the AM machine, as shown in the step 0 in Figs. 9 and 12, respectively. However, significant residual forces are reacted through the baseplate, which are released when the reinforced plate is removed from the baseplate inducing significant deformation of the plates and approximately doubling their flatness. There is also an accompanying change in the shape as shown in Figs. 9 and 12. For the plate built in the landscape orientation (Fig. 9), the out-of-plane displacements during the incremental release from the baseplate are substantially larger in the bottom half of the plate than in the top half. This is unsurprising because the effect of the residual forces reacted through the baseplate would be expected to be greater adjacent to the baseplate and to dissipate with distance from the baseplate. Hence, the release of these forces as the connections to the baseplate are cut would be expected to cause greater deformation adjacent to the cut edge. The same phenomenon is present in the reinforced plate built in portrait orientation (Fig. 12); however,

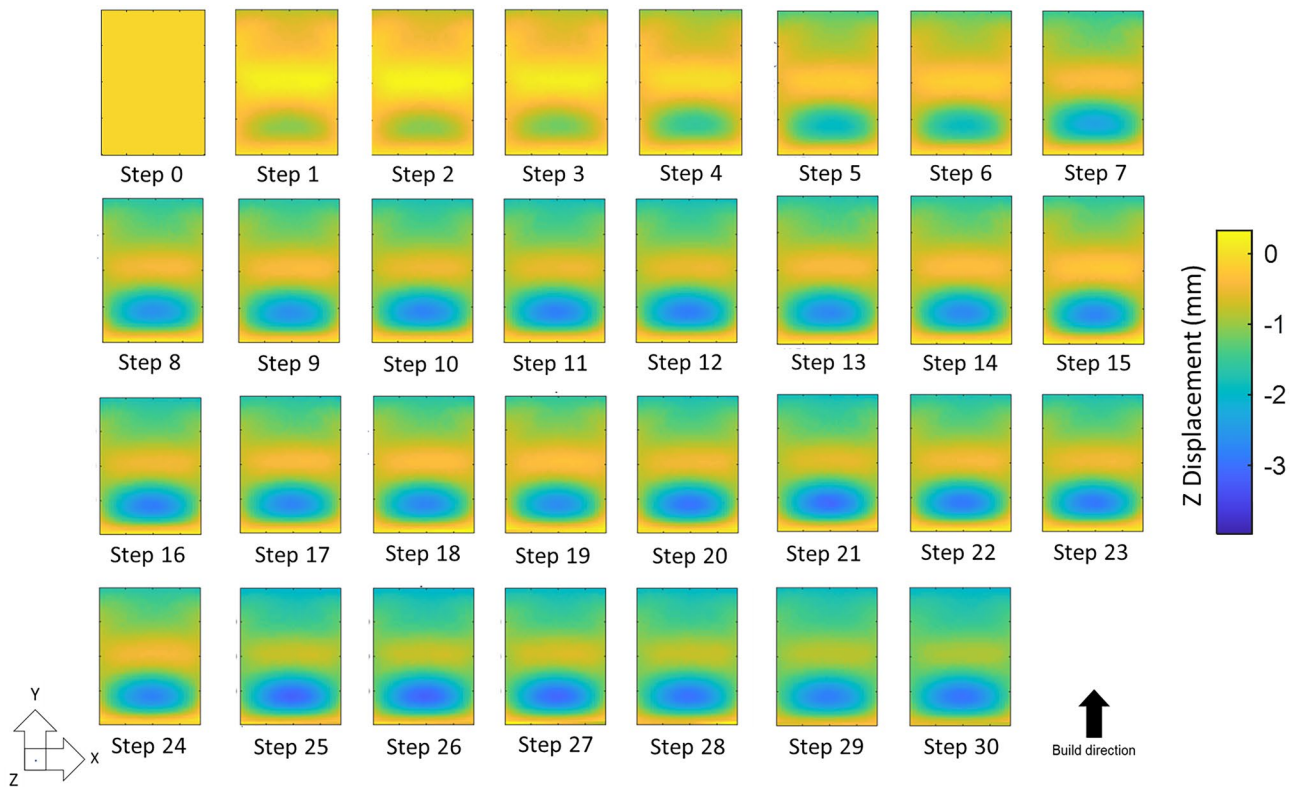


**Fig. 12** Out-of-plane displacements measured at each increment of 5 mm release from baseplate (odd numbers on right) for edge-reinforced portrait plate with in-plane and out-of-plane additional buttresses (see

geometry in Fig. 11). The displacements are relative to initial shape of the plate on the baseplate at the end of the build cycle and measured on the front face (step 0)

the magnitude of the difference between the displacements at the top and bottom of the plate is much smaller probably due to the shorter horizontal dimension and closer proximity of vertical portions of the edge-reinforcement. Based on prior work [6], it would be expected that the reinforced plate exerts compressive forces vertically on the baseplate in the centre of its bottom edge and tensile forces at the ends of its bottom edge. Hence, from Newton’s third law, the baseplate exerts tensile forces at the centre of the edge and compressive forces at the ends. The release of these forces would tend to make the bottom edge of the reinforced plate bend upwards in the centre to form a catenary orientated like an arch; however, the in-plane stiffness of the thin plate is very high compared to its out-of-plane stiffness due to its geometry and, as a consequence, the plate deforms out-of-plane forming a domed shape. The deformation is more severe in the bottom half of the plate than in the top half (see Figs. 9 and 12) due to the proximity to the baseplate and the larger influence of the residual forces reacted through the baseplate as described above. For the plate built in the landscape orientation, the end result is a domed shape that is broader at the bottom of the plate than the top. Whereas for the plate built in the portrait orientation, the result is a change in shape from a central negative z-direction dimple

with positive z-direction dimples above and below (see Fig. 11) to a single negative direction dimple with a single positive direction one above. In the portrait orientation, the release of constraining forces from the baseplate removes the lower dimple, deepens the central one and relaxes the top one. We also investigated whether the resulting shapes in the portrait and landscape orientation builds were connected to buckling characteristics of the plate geometries. However, it is important to note that both the development of residual stresses during the build as material is being added and the development of the final plate shape as baseplate supports are being severed are gradual processes. Thus, a global buckling response after the event (i.e. after build and after support release) seems unlikely. However, the final shape of the plates exhibited snap-back behaviour in most cases, i.e. they were bi-stable structures with two mechanically stable configurations.

The smaller area and aspect ratio of the layers built in the portrait orientation compared to the landscape orientation will have resulted in the laser revisiting each region of the part more quickly. This will have increased the rate of energy input per unit volume. However, previous work has shown that, above a minimum threshold, the rate of energy input has an insignificant effect on the level of residual stresses.

Hence, it seems likely that the differences in shape the plates built in the landscape and portrait orientations result from geometric effects associated with constraining the long and short edges respectively via their attachment to the baseplate; as well as from the differential thermal strains between layers in the longitudinal or transverse directions respectively. The larger number of layers required to build the reinforced plate in the portrait orientation appears to make the plate more susceptible to delamination as demonstrated by the requirement to use in-plane buttresses to prevent delamination, which were not necessary for the plates built in the landscape orientation. The smaller aspect ratio (i.e. 130:1 compared to 230:1) of the layers built in portrait orientation led to smaller out-of-displacements and flatter plates.

It is difficult to predict from the data acquired whether the use of buttresses would be effective for other aspect ratios and in other materials, though it seems likely. However, the data presented in Figs. 8, 9, 11 and 12 should be invaluable in future work to develop computational models of the build process and the associated development of residual stresses.

## 5 Conclusions

Geometrically reinforced thin plates have been built using laser-powder bed fusion (L-PBF) and their shapes measured using stereoscopic digital image correlation before and after release from the baseplate of the AM machine. The results were used to draw the following conclusions:

1. Residual stresses induced by additive manufacturing cause potentially severe out-of-plane deformations which have been evaluated using digital image correlation before, during and after release from the baseplate.
2. Stripe scan strategy induced lower magnitudes of out-of-plane deformation than Meander scan strategy.
3. An enveloping support structure reduced the magnitude of out-of-plane deformation to less than 5% of in-plane dimensions; however, the support increased the build time substantially, it was difficult to remove and it led to a substantial amount of material being scrapped.
4. Buttress supports to the reinforced edges of the thin plate reduced out-of-plane deformation to less than 5% of in-plane dimensions, were quick to build and remove and minimised waste; however, they needed to be designed carefully.
5. Plates built in landscape orientation required out-of-plane buttresses while those built in portrait orientation required both in-plane and out-of-plane buttresses. Out-of-plane deformation increased on release from the baseplate but was mitigated by incremental release.
6. Building reinforced thin plates in the portrait orientation led to small maximum out-of-plane deformation (about

4.6 mm) compared to landscape orientation (about 5.5 mm).

**Author contribution** John Lambros, Eann Patterson and Chris Sutcliffe contributed to the study conception and design. Material preparation, data collection and analysis were performed by Rodrigo Magana-Carranza. The first draft of the manuscript was written by Eann Patterson, and all authors commented on previous versions of the manuscript. All authors read and approved the final manuscript.

**Funding** The research was supported by grants from both the EPSRC (grant no. EP/T013141/1) in UK and NSF CMMI (grant no. 20–27082) in the USA. The authors are grateful to funders for providing the resources for the research and to the University of Liverpool for access to facilities to perform the research.

## Declarations

**Conflict of interest** The authors declare no competing interests.

**Open Access** This article is licensed under a Creative Commons Attribution 4.0 International License, which permits use, sharing, adaptation, distribution and reproduction in any medium or format, as long as you give appropriate credit to the original author(s) and the source, provide a link to the Creative Commons licence, and indicate if changes were made. The images or other third party material in this article are included in the article's Creative Commons licence, unless indicated otherwise in a credit line to the material. If material is not included in the article's Creative Commons licence and your intended use is not permitted by statutory regulation or exceeds the permitted use, you will need to obtain permission directly from the copyright holder. To view a copy of this licence, visit <http://creativecommons.org/licenses/by/4.0/>.

## References

1. Curtis JD, Hanna SD, Patterson EA, Taroni M (2003) On the use of stereolithography for the manufacture of photoelastic models. *Exp Mech* 43(2):148–162
2. Silva AS, Sebastian CM, Lambros J, Patterson EA (2019) High temperature modal analysis of a non-uniformly heated rectangular plate: experiments and simulations. *J Sound Vib* 443:397–410
3. Lopez-Alba E, Sebastian CM, Silva ACS, Patterson EA (2019) Experimental study of mode shifting in an asymmetrically heated rectangular plate. *J Sound Vib* 439:241–250
4. Silva ACS, Lambros J, Garner DM, Patterson EA (2020) Dynamic response of a thermally stressed plate with reinforced edges. *Exp Mech* 60:81–92
5. Withers P (2007) Residual stress and its role in failure. *Rep Prog Phys* 70(12):2211
6. Li C, Liu ZY, Fang XY, Guo YB (2018) Residual stress in metal additive manufacturing. *Procedia CIRP* 71:348–353
7. Bartlett JL, Li X (2019) An overview of residual stresses in metal powder bed fusion. *Addit Manuf* 27:131–149
8. Mercelis P, Kruth JP (2006) Residual stresses in selective laser sintering and selective laser melting. *Rapid Prototyp J* 12(5):254–265
9. Qian W, Wu S, Wu Z, Ahmed S, Zhang W, Qian G, Withers PJ (2022) In situ X-ray imaging of fatigue crack growth from multiple defects in additively manufactured AlSi10Mg alloy. *Int J Fatigue* 155:106616
10. Anderson LS, Venter AM, Vrancken B, Marais D, Van Humbeeck J, Becker TH (2018) Investigating the residual stress distribution

- in selective laser melting produced Ti-6Al-4V using neutron diffraction. In *Mater Res Proc* 4:73–78
11. Magana-Carranza R, Robinson J, Ashton I, Fox P, Sutcliffe C, Patterson E (2021) A novel device for in-situ force measurements during laser powder bed fusion (L-PBF). *Rapid Prototyp J* 27(7):1423–1431
  12. Magana-Carranza R, Sutcliffe CJ, Patterson EA (2021) The effect of processing parameters and material properties on residual forces induced in Laser Powder Bed Fusion (L-PBF). *Addit Manuf* 46:102192
  13. Gibson I, Rosen DW, Stucker B, Khorasani M (2014). *Additive manufacturing technologies*. 2014, Springer: New York, USA
  14. Wohlers T, Gornet T (2014) History of additive manufacturing Wohlers report 24(2014):118
  15. [https://www.carpenteradditive.com/hubfs/Resources/Data%20Sheets/PowderRange\\_625\\_Datasheet.pdf](https://www.carpenteradditive.com/hubfs/Resources/Data%20Sheets/PowderRange_625_Datasheet.pdf) [last Accessed 15 Aug 2022]
  16. Kruth JP, Deckers J, Yasa E, Wauthlé R (2012) Assessing and comparing influencing factors of residual stresses in selective laser melting using a novel analysis method. *Proc Inst Mech Eng Part B J Eng Manuf* 226(6):980–991
  17. Shiomi M, Osakada K, Nakamura K, Yamashita T, Abe F (2004) Residual stress within metallic model made by selective laser melting process. *CIRP Ann* 53(1):195–198
  18. Hild F, Roux S (2013) Digital image correlation, in optical methods for solid mechanics: a full-field approach, Rastogi PK & Hack E (editors), John Wiley & Sons, New York
  19. Thomas GG (1974) *Engineering metrology*. Butterworths, London

**Publisher's Note** Springer Nature remains neutral with regard to jurisdictional claims in published maps and institutional affiliations.